SLAC – PUB – 3728
July 1985
(E)

PLANS FOR POLARIZED BEAMS AT THE SLC*

CHARLES Y. PRESCOTT

Stanford Linear Accelerator Center
Stanford University, Stanford, California, 94305

ABSTRACT

Precision tests of the electroweak interactions will soon be possible at the SLC and LEP. The SLC will be capable of providing longitudinal polarization of one incoming beam, the electrons, for such tests. Plans at the SLC to provide and monitor these beams are described, and some physics objectives are discussed.

Invited talk presented at the Workshop on Tests of
Electroweak Theories, Polarized Processes, and Other Phenomena
Trieste, Italy, June 10-12, 1985

---

* Work supported by the Department of Energy, contract DE-AC03-76SF00515.

1. INTRODUCTION

The startup of the SLC and LEP machines in the next several years will mark the beginning of extensive and precise tests of the electroweak interactions. The expected luminosities of SLC, with a design goal of 6×10^{30} cm^{-2} sec^{-1}, and LEP, with a design goal of 1.6×10^{31} cm^{-2} sec^{-1}, translate into approximately 3×10^{6} Z°'s per year for each experiment or detector. The SLC will have one interaction region and one active detector (Mark II or SLD) and LEP will have four (ALEPH/OPAL/DELPHI/L3). Each are capable of accumulating more than 10^{7} Z°'s in a few years work. With such large samples of data, precise tests of the standard decay modes and extensive searches for rare decays will take place. At the SLC, the work can be placed in three general categories: (i) tests of the standard model predictions, roughly an order of magnitude better than the present experimental tests; (ii) searches for new phenomena, some compatible with the standard model, some not; and (iii) development of new techniques for a future linear collider, including studies of beam-beam interactions, beam-linac interactions, and beam polarization.

2. TESTING THE STANDARD MODEL

The first and most direct measurement to be made at the SLC will likely be the study of the mass and width of the Z°. These early tests will serve to map out the cross section for several purposes. First, the study of the Z° depends on the high rate of production that occurs at the peak of the resonance. Finding the peak and measuring it's cross section will have early priority in an SLC program. The measurement of the width will also result from a scan of the machine energy. From mapping the shape of the Z°, the free parameter of the electroweak theory, $sin^2\theta_W$, will be determined. This parameter can be related to the mass by

$$M(Z^{\circ}) = \left[\frac{\pi\alpha}{\sqrt{2}G_F}\right]^{1/2} \frac{1+\Delta_{\mathrm{WEAK}}}{\sin\theta_W \ \cos\theta_W}$$

where Δ_{WEAK} expresses the effect of higher order electroweak corrections, and has the value of $0.070 \pm .002$.[1]

The mass of the $Z°$ will be measured by raising the beam energy in successive steps, measuring the total event yields and and luminosities, thereby mapping out the line shape. Since the cross sections are large near the $Z°$ resonance, statistical errors should be small compared to systematic errors, and errors in the mass of the $Z°$ will come from calibration errors in beam energy, luminosity uncertainties, and uncertainties in line shape due to radiative processes.

At the SLC, beam energies will be known by mapping of the magnetic fields in the transport lines. Careful work should give accuracies of perhaps $\pm 0.2\%$ for each beam. This corresponds to $\Delta M(Z°) = \pm 130\, MeV$, and $\Delta \sin^2 \theta_W \approx \pm .0008$. This measurement will be approximately one order of magnitude improvement on the present low energy measurements of this parameter. Calibration of the SLC transport lines is possible using precession of spin in polarized beams, and further reduction in systematic errors is possible. Similar techniques apply to LEP, where spin resonances can be measured with great accuracy. If sufficient attention to other systematics is given, LEP ultimately can make the best measurement of the fundamental electroweak parameter, $\sin^2 \theta_W$.

Measurement of the $Z°$ mass serves to fix the standard model parameters, but alone does not provide a test, since apriori these values are undetermined. Further measurements other than the mass are required to begin the precise tests that are wanted. Examples of further observables are: (i) the width of the $Z°$, (ii) the mass of the W, and (iii) measurement of couplings to the quarks and leptons. The energy of the SLC will be limited to $\sqrt{s} \approx 100\, GeV$, at least for the near future. Hence the SLC cannot produce $W^{\pm}$ pairs, and single W production is too small to provide experimental information. LEP will later be capable of studying $W^{\pm}$ pairs, and accurate W mass measurements can result. However in the near term, other means can be used to test the electroweak theory. The measurement of the width of the $Z°$ is interesting in its own right, but probably lacks sufficient accuracy to challenge the electroweak theory. Observables which are sensitive to fermion couplings do provide sensitivity at a sufficient level to make interesting tests possible. These observables include A_{FB}, the forward-backward charge asymmetries, A_{LR}, the longitudinal spin-flip asymmetry, and P_f, the final state polarization of the fermions. These observables have been studied and discussed in numerous reports. For this talk, I wish to focus on A_{LR}, which is an observable that will be available to experimenters when the SLC runs with longitudinally polarized electrons beams.

The polarized beam asymmetry A_{LR} is defined to be

$$A_{LR} = \frac{\sigma_L - \sigma_R}{\sigma_L + \sigma_R}$$

where $\sigma_{L(R)}$ is the cross section for a process or processes of interest where the incident electron beam is in a state of $-(+)$ helicity. This asymmetry can be measured rather easily in polarized beams at the SLC, where individual linac pulses of $+$ or $-$ helicity are interleaved and tagged. Systematic uncertainties, such as luminosity and detector uncertainties, largely cancel . The systematic errors tend to be small, and at the Z° where counting rates are high, statistical errors can also be small in many channels. Hence, the experimental errors on A_{LR} can be expected to be quite good.

If one looks closely at the relationships to neutral current couplings, the polarization asymmetry is seen to depend *linearly* on the vector couplings to the Z° (which are proportional to 1-4$\sin^2\theta_W$ and tend to be small), while the charge asymmetries depend *quadratically* on this parameter. In many theories, the effect of "new physics" will manifest itself through propagator effects and influence the couplings. Sensitivity to small effects is greater in A_{LR} than in A_{FB} because of the linear, rather than quadratic, dependence on the small vector couplings. It appears that A_{LR} is the more sensitive asymmetry to use for searches of new physics hidden in the propagator effects associated with the Z°.

Figures 1-3 show the expected influence, in lowest order, of longitudinal polarization on total cross sections, forward-backward asymmetries, and on final state polarizations. The examples shown are: (1) hadron production for three beam polarizations, + helicity (e_R), − helicity (e_L), and unpolarized (0); (2a-2c) charge asymmetries for $u\bar{u}$ quark pairs, $d\bar{d}$ quark pairs, and $\mu^{\pm}$ pairs; and (3) final state lepton (i.e., τ) polarization. Through universality, these relationships are valid for the other families of quarks and leptons. We see that charge asymmetries are substantially enhanced, or modulated, by longitudinal polarization. Measurement of total cross section asymmetries offers the best possible statistical errors and, when combined with the low systematic errors, should yield excellent measurements of the electron coupling to the Z°. It is the latter measurement that is the best alternate measurement if $\sin^2\theta_W$, comparable to that from the Z° mass, and should provide an accurate test of the electroweak theory.

As discussed in a following section, the experimental errors should be smaller than ±.005 on A_{LR}. Figure 4[2] compares this experimental error with the influence of higher order electroweak corrections, after QED effects have been considered. We see that the experimental errors are good enough to require that higher order electroweak effects be properly included.

Figures 5,6[3] and 7,[4] show two examples of hypothesized new processes falling outside our present standard model based on three families of quarks and leptons. These figures illustrate that new phenomena can modify the observable quantity A_{LR} well beyond the experimental resolution of ±.005. These two graphs, and others like them, tell the experimental physicist the target to seek when designing precision experiments. The A_{LR} asymmetry is sensitive to the mass of the Higgs boson, assuming the standard model Higgs exists, and if so, may lead to a substantial theoretical uncertainty if the Higgs remains hidden. Or perhaps this dependence may serve to better define the range of the allowed masses for the Higgs. In any event, polarized beams are a fundamentally interesting probe of the electroweak interactions.

3. EXPERIMENTAL TECHNIQUES

I would now like to describe various aspects of the process by which we plan to obtain polarized beams. These aspects include production, acceleration, transportation, and monitoring. Electrons, but not positrons, are born with longitudinal polarization. This process has been previously used at SLAC.[5] Briefly, one constructs an electron gun with a cathode of gallium arsenide which has been properly coated with cesium-oxygen layers. Illuminating the cathode with circularly polarized laser light of the appropriate wavelength (in the visible red, around 780 nm) leads to the photoemission of longitudinally polarized electrons. With properly prepared gallium arsenide cathodes, high quantum efficiencies are obtained, and modest laser pulses provide large instantaneous currents, ideal for injection into pulsed linacs, such as the SLC. Currents from appropriately designed guns should provide full intensity required to run the SLC at its design luminosity. Polarization of electrons from gallium arsenide has been measured around 40 to 45%, showing some modest depolarization from the expected 50%. The helicity of the electrons can be easily and rapidly reversed, leading to a pattern of helicities set by experimental needs. Typically individual machine pulses have randomly set helicities. Each pulse is tagged by $+1$, -1, or 0, and can be used or ignored by the experimenter depending on his inclinations and the problem under study. The magnitude of the polarization can depend on a number of factors, including depolarization effects. It must be measured experimentally, and monitors to do this will be described shortly.

Higher polarization is being sought, through studies of alternatives to gallium arsenide as a cathode material. It is reasonable to hope for increased polarization using these new materials. Higher polarization will significantly benefit the experiments through reduced systematic errors.

Depolarization of the beam can occur at several points in the acceleration and transportation of the beams. The linear accelerator does not significantly depolarize beams, but beams must pass into and back out of the damping rings (the small storage rings for reducing the beam phase space). These rings (one for the electrons, one for the positrons) hold the beams for one or two machine pulse periods, 5.3 *msec*. To prevent spin depolarization, the spin must be oriented to point in the direction of the magnetic guide field, that is normal to the plane of the ring. A solenoidal field of 6.3 Tesla-meters rotates the spin to this orientation when placed appropriately in the 1.2 GeV input line from the linac to the damping ring. In the output line that returns the beam to the linac, two similar solenoids will exist to return the spin to longitudinal, or any other orientation desired. Depolarization of spin in the ring will be studied in the year soon after operation of the SLC has settled down.

Depolarization in the arcs which deliver beams to the experimental hall also is expected to occur. Spin motion consists of a rapid precession in the horizontal plane, due to the electron g-2 term, and a similar but slower rolling in the vertical plane because the SLC arcs have vertical deflections to follow the local terrain. The result is a spin orientation which can have somewhat different components along all axes for different beam energies. The flexibility in the spin control comes from two solenoids at the output of the of the damping ring. It is planned to measure and tune the spin to longitudinal orientation at the experiments.

Because of the finite beam energy spread, different energy particles in the beam precess different amounts. Estimates show that the energy spread of $\pm 0.5\%$ leads to a 14% depolarization, which is an acceptable amount. More recent design goals for the SLC have reduced the energy spread to $\pm 0.2\%$, and the corresponding depolarization will be significantly lower. Synchrotron radiation causes further fluctuations in beam orbits, and contributes an additional, but small, amount to the energy spread. Also, when e^+ and e^- beams pass through one another, the orbits (and the spin vectors) undergo motion as particles see the strong fields of the other bunch. These effects further contribute small amounts to the total depolarization. Such effects can be estimated, but depend on the various beam conditions, some of which will vary during data collection. The conclusion to draw from the above discussion is that beam polarization must be *measured* by the experimenters.

To give a more quantitative feeling for the accuracies possible for A_{LR}, consider the following experimental situation. Suppose one wishes to measure the spin-flip asymmetry A_{LR} in $e^+ \, e^-(pol) \rightarrow \mu^+ \, \mu^-$ at the Z° peak, with $\approx 50\%$ polarized beam. The spin-flip asymmetry is

$$A_{LR} = \frac{1}{P_e} \left[\frac{N_L - N_R}{N_L + N_R} \right]$$

where $N_R(N_L)$ is the total number of μ-pairs detected in all 4π solid angle, for right-handed (left-handed) incident electron polarization. The error in A_{LR} can be expressed as

$$\left[\Delta A_{LR}\right]^2 \approx \left[\frac{\Delta P_e}{P_e} A_{LR} \right]^2 + \frac{(1 - A_{LR}^2)^2}{2P_e^2[N_R + N_L]}$$

where the first term is the main systematic error coming from the uncertainty $\Delta P_e/P_e$ term, and the statistical error is given by the second term. For a sample of 10^6 Z°'s produced, 3×10^4 will be seen in the $\mu^+\mu^-$ final state. The statistical error for $P_e \approx 50\%$ is estimated to be $\pm$ 0.008. Incorporating other final states, say τ pairs, can further reduce the statistical errors.

Systematic errors on ΔA_{LR} arise from various sources. The dominant term comes from the beam polarization uncertainty $\Delta P_e/P_e$, and is proportional to the asymmetry A_{LR}, which is expected to be small. A value of $\Delta P_e/P_e = .05$ was achieved in previous work at SLAC. The expected value of $A_{LR} \approx 0.2$ gives a systematic error of ± 0.01. To reduce the systematic terms, improved polarization monitoring, and higher beam polarization help. With some careful work, it is expected to be able to reach the $\pm .003$ to $\pm .005$ level on A_{LR}.

Polarization monitoring requires special experiments. The two types of monitors being actively considered are both based on QED processes which have large spin-dependent terms. Measurement of the beam polarization is achieved by measuring the spin-dependent terms, and comparing with values calculated for 100% polarization. The systematic errors for the two techniques are important to understand. They are different in the two techniques, and hence provide a cross check on the results. Statistical errors are insignificant in comparison to systematic errors.

The first technique considered is Møller scattering, which is the process

$$e + e \rightarrow e + e$$

The incident electron is high energy, while the second electron is at rest. Both incident and target electron are polarized, with spins parallel or anti-parallel for longitudinal spins. The scattered electrons go forward and are analyzed with a magnetic field and a detector. The dispersion in angle and momenta define the two-body process. Detection of the scattered electrons permits computing the asymmetry

$$A_{ee} = \frac{\sigma_p - \sigma_a}{\sigma_p + \sigma_a}$$

where $\sigma_p(\sigma_a)$ is the Møller cross section for parallel (anti-parallel) spins. For a 100% polarized target, this value is large, $A_{ee} = 7/9$. For a polarized target of magnetized iron, only 2 out of 26 electrons are aligned. The expected asymmetry for magnetically saturated iron is thus $\approx 7/9 \times 2/26 \approx 6\%$. Careful measurements of the iron magnetization and geometry permit the experimental A_{ee} for 100% beam polarization to be estimated to reasonably high accuracy, $\pm 1\%$ of the 6%. Figure 8 shows the layout of such a monitor which was used at SLAC in 1978 with polarized beams. The Møller signal from the 1978 data is shown in Figure 9(a), and the corresponding asymmetry in Figure 9(b). The accuracy of the polarization measurement is limited by a background from e-Fe nucleus scattering. Subtraction of the background leads to an error of about $\pm 5\%$ for $\Delta P_e/P_e$. Counting rates are very high, and the Møller system is an excellent monitor, on a minute-by-minute basis, of the polarization.

A second, perhaps more accurate, technique uses Compton scattering of a polarized laser beam from the incident polarized electron beam:

$$\gamma + e^- \rightarrow \gamma + e^-$$

This process certainly bypasses the problems of a background from a fixed target. It is a pure QED process, and has the potential of being a highly precise measure of beam polarization. The backscattered photon has a maximum energy given by $k_{\max} = 4\gamma^2 k/(1 + 4\gamma k/m_e)$, where k is the laser photon energy and $\gamma = E/m_e$ for the electron. Both the scattered and the outgoing electron go forward. the outgoing electron has only a fraction of the incident electron energy. Measurement of electron polarization proceeds somewhat like that for Møller scattering, where one measures the asymmetry

$$A_{e\gamma} = \frac{\sigma_p(e\gamma) - \sigma_a(e\gamma)}{\sigma_p(e\gamma) + \sigma_a(e\gamma)}$$

by comparing the backward part of the cross sections for parallel and anti-parallel spins. In this case, the circular polarization of the photon replaces the longitudinal polarization in the Møller target. Figure 10 illustrates schematically the arrangement. Cross sections can be measured by detecting the backscattered photon, or final electron. At the SLC, the latter is probably preferred, because the final electron can be swept out of the beam by a magnet, as illustrated. Asymmetries are relatively large and readily computed, but depend on the kinematic parameters. Backgrounds should be small, counting rates high, and polarization measurements quick. One expects polarized Compton scattering to provide accurate measurements of electron beam polarization.

One final comment should be added. Accurate measurement of spin precession of electrons can serve to calibrate the energy of the SLC arcs. The spin precession depends linearly in the beam energy. In passing through the arc magnets, the spin undergoes approximately 26 full revolutions at 45 GeV. Measurement to $\pm 10°$ at the interaction region corresponds to $\Delta E/E \approx \pm 0.1\%$. This technique provides a possible means to improve SLC's energy precision. The e^+ beam cannot be directly measured by this technique since the e^+'s are unpolarized. However measurement of colinearity of $\mu\mu$ or ee pairs readily establishes the e^+ energy relative to the e^- beam.

4. CONCLUSIONS

Polarized beams for the SLC are planned to begin soon after sufficient luminosity is achieved to provide physics experiments with data. The longitudinal polarization asymmetries are sensitive to new physics processes outside the standard model. Experimental accuracies should be good enough to look for effects of new physics through influences on these asymmetries. Accurate monitoring of beam polarization is important to asymmetry measurements, and are being planned for the SLC.

REFERENCES

1. G. Altarelli, et. al. LEP Yellow Book, CERN 1985.
2. B. W. Lynn and R. G. Stuart, Nucl. Phys. **B253**, 216, 1985.
3. B. W. Lynn, M. E. Peskin, and R. G. Stuart, SLAC-PUB-3725 (1985), submitted to Proceedings of the LEP Physics Workshop, CERN Report 1985, (LEP "yellow book").
4. B. W. Lynn, SLAC-PUB-3358, 1984.
5. C. K. Sinclair, Proceedings of the conference on High Energy Physics with Polarized beams and Targets Argonne, 1976.

FIGURE CAPTIONS

Fig. 1. Total cross section ratio R versus center-of-mass energy for left-handed (e_L), right-handed (e_R), and unpolarized (0) beams.

Fig. 2. The charge asymmetry A_{FB} versus center-of-mass energy for left-handed (e_L), right-handed (e_R), and unpolarized (0) beams.

Fig. 3. Final state lepton polarization (for the τ) versus center-of-mass energy for left-handed (e_L), right-handed (e_R), and unpolarized (0) beams.

Fig. 4. A_{LR} versus center-of-mass energy with and without electroweak radiative corrections: (- - -) are tree-level terms only; (.....) are 1-loop QED corrections only; (——) are full electroweak corrections to 1-loop (see Ref. 2).

Fig. 5. The corrections beyond the standard electroweak ones, δA_{LR}, from an extra heavy quark doublet (U, D); the ratio M_D/M_U is shown for the values 0.2, 0.5, 0.8, and 1.0 (see Ref. 3).

Fig. 6. The corrections beyond the standard electroweak ones, δA_{LR}, for an extra heavy lepton doublet (ν, L); curves for four values of the ratio M_ν/M_L are shown (see Ref. 3).

Fig. 7. The corrections beyond the standard electroweak ones, δA_{LR}, versus gravitino mass in a supergravity model (see Ref. 4).

Fig. 8. A schematic view of a Møller polarimeter, consisting of a polarized iron target, a septum magnet, and an electron detector-hodoscope.

Fig. 9. Møller scattering data from SLAC (1978); (a) the cross section versus scattering angle (scales relative) showing the Møller peak on a background from e-Fe scattering; and (b) the asymmetry (on an absolute scale corresponding to approximately 40% polarization.

Fig. 10. Schematic of a Compton polarimeter not to scale, showing a polarized laser beam colliding with the incident electron beam. Incoming circularly polarized laser light intercepts the electron beam downstream from the interaction point (IP) after it passes through the experimental hall. Backscattered photons and and associated electrons resulting from the interactions move with the electron beam until a final focus bend magnet, and then are separated from it, where they can be analyzed. Measurement of the Compton asymmetry, $A_{e\gamma}$, in an electron detector serves to determine the incident polarization.

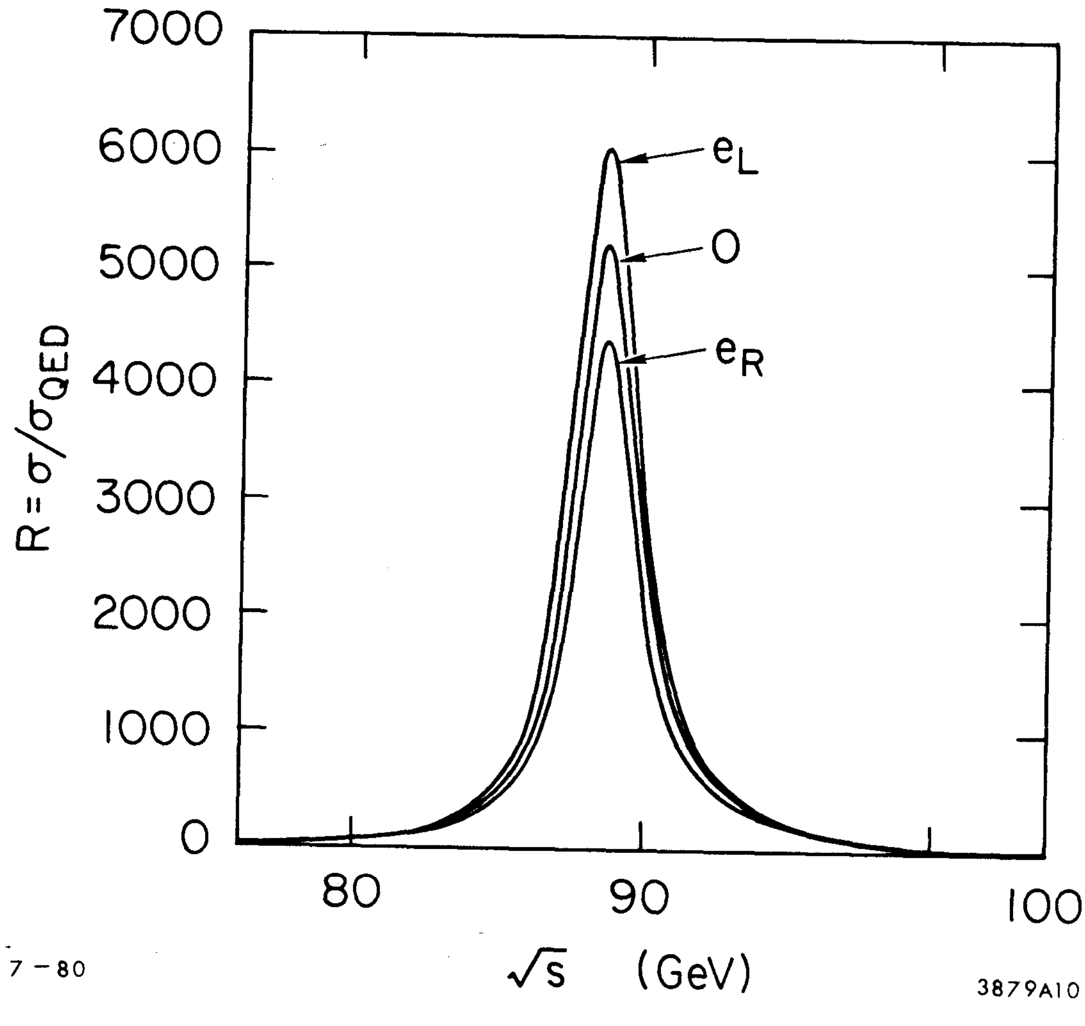

7000
6000
5000
4000
3000
2000
1000
0
$R = \sigma/\sigma_{QED}$
e_L
0
e_R
80
90
100
$\sqrt{s}$ (GeV)
7 – 80
3879A10

Fig. 1

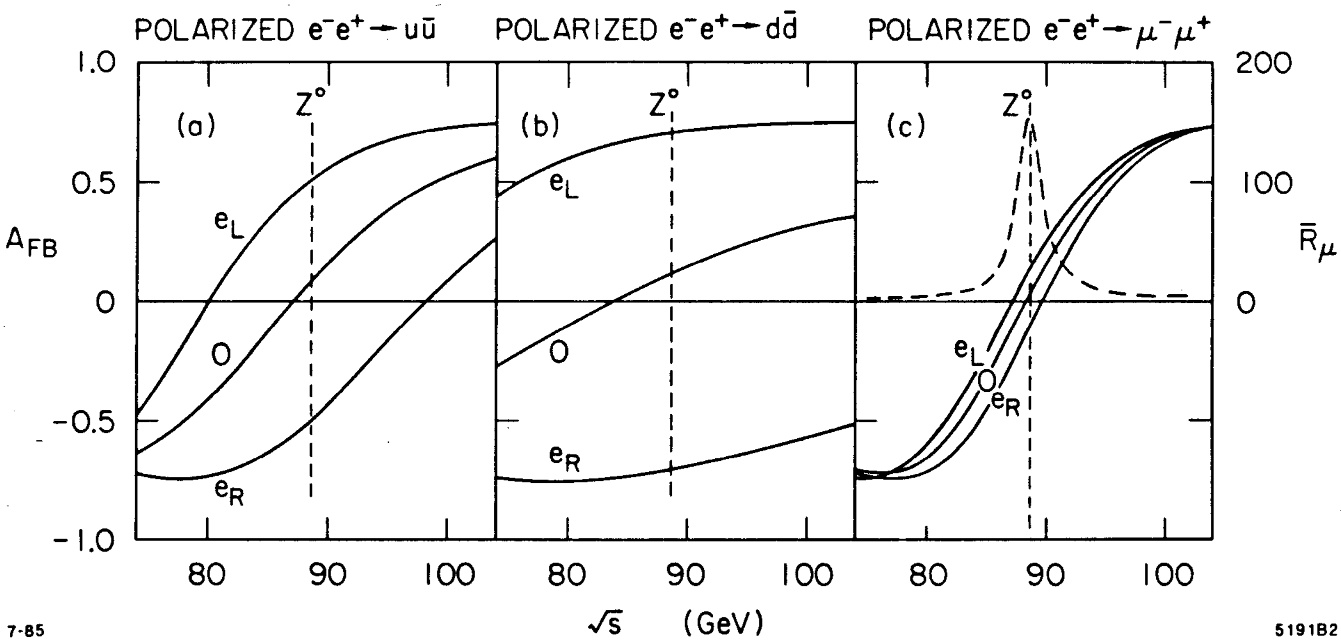

POLARIZED $e^-e^+ \to u\bar{u}$
POLARIZED $e^-e^+ \to d\bar{d}$
POLARIZED $e^-e^+ \to \mu^-\mu^+$
A_{FB}
$\bar{R}_\mu$
(a)
(b)
(c)
Z°
e_L
O
e_R
1.0
0.5
0
-0.5
-1.0
200
100
80
90
100
$\sqrt{s}$ (GeV)
7-85
5191B2

Fig. 2

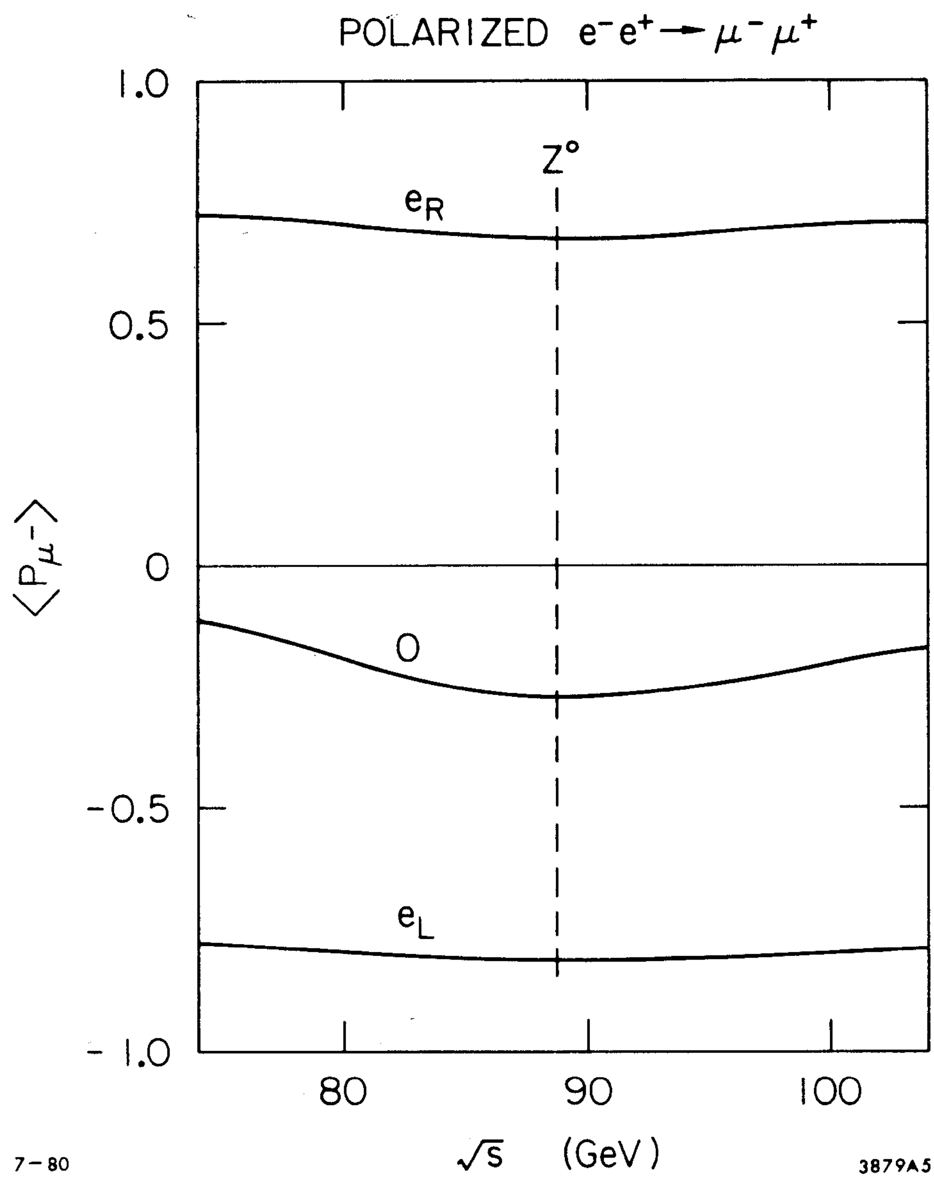
POLARIZED e⁻e⁺ → μ⁻μ⁺
1.0
0.5
0
-0.5
- 1.0
Z°
e_R
O
e_L
⟨P_μ⁻⟩
80
90
100
√s (GeV)
7-80
3879A5

Fig. 3

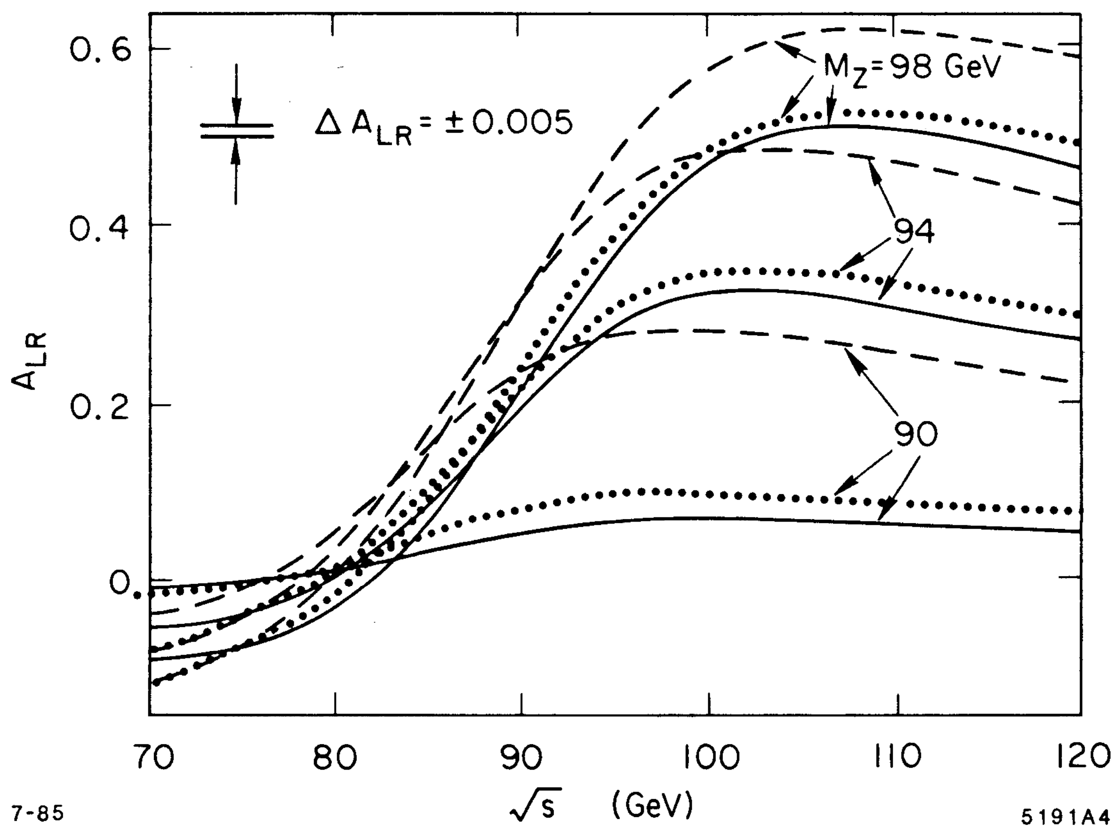

0.6
0.4
0.2
0.
A_{LR}
$\Delta A_{LR} = \pm 0.005$
M_Z=98 GeV
94
90
70
80
90
100
110
120
$\sqrt{s}$ (GeV)
7-85
5191A4

Fig. 4

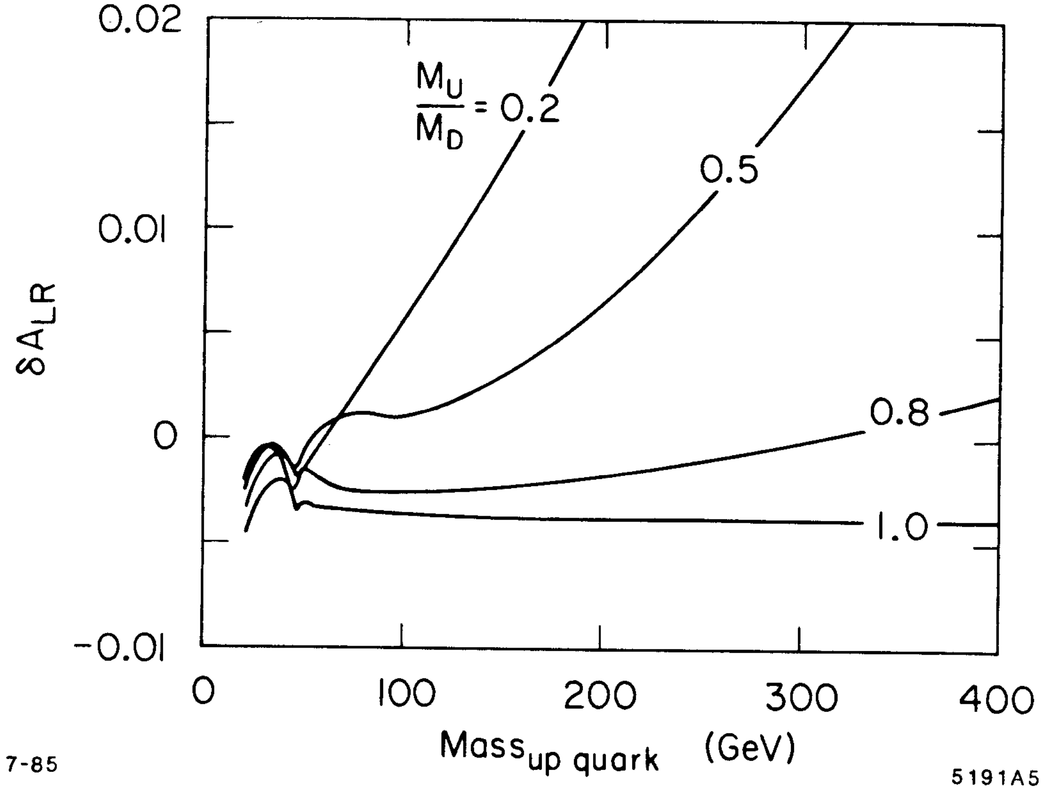
0.02
0.01
0
-0.01
δA_{LR}
$\frac{M_U}{M_D}$ = 0.2
0.5
0.8
1.0
0
100
200
300
400
Mass$_{up\ quark}$ (GeV)
7-85
5191A5

Fig. 5

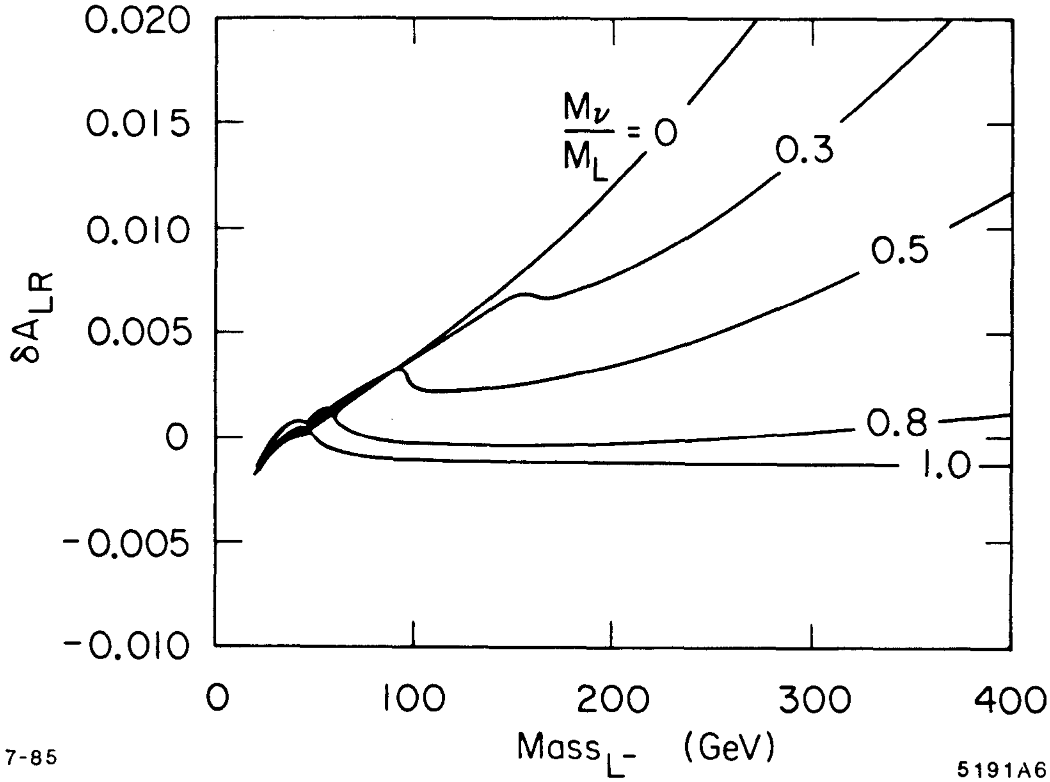

0.020
0.015
0.010
0.005
0
-0.005
-0.010
δA_{LR}
$\frac{M_\nu}{M_L} = 0$
0.3
0.5
0.8
1.0
0
100
200
300
400
Mass_{L^-} (GeV)
7-85
5191A6

Fig. 6

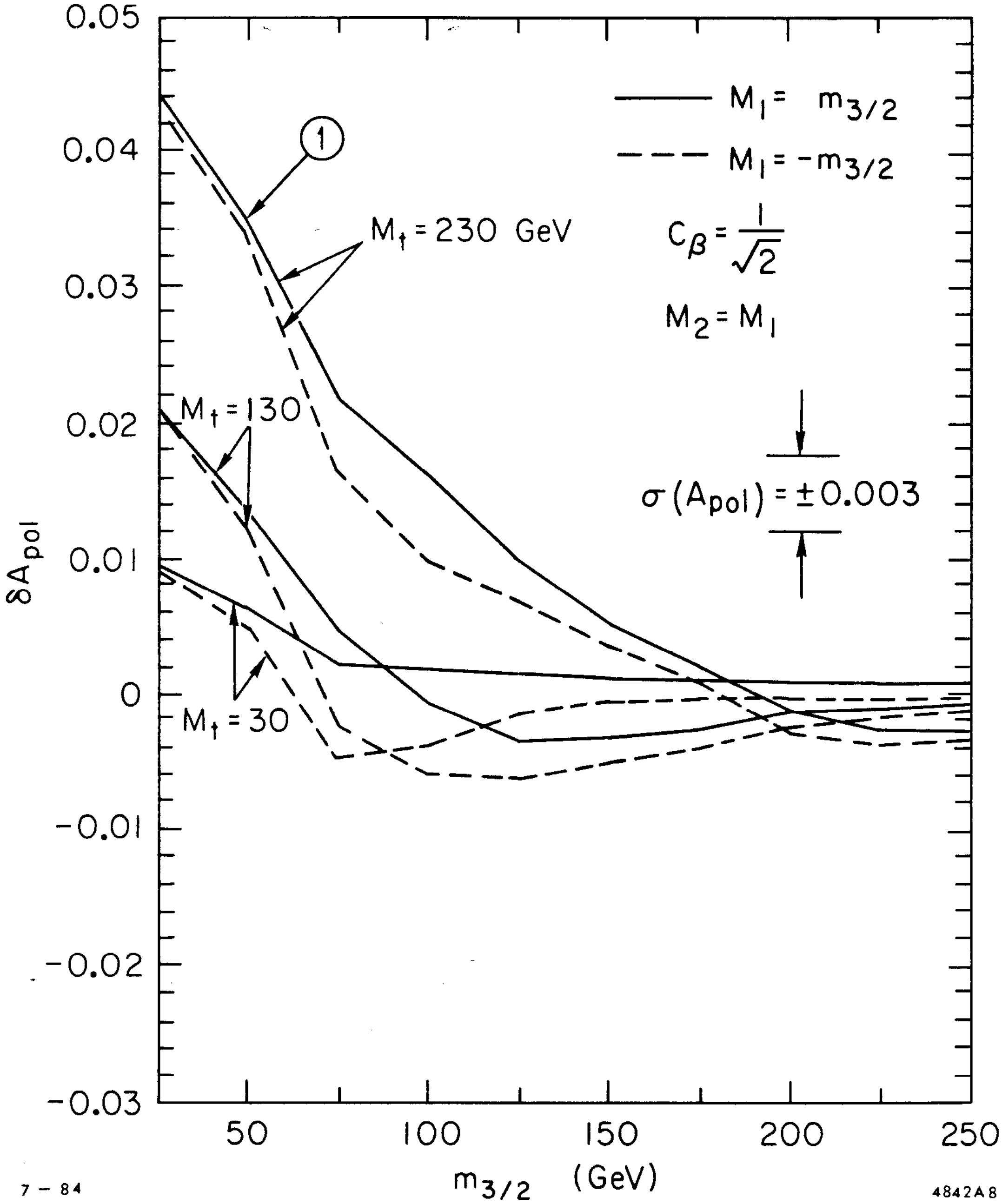

0.05
0.04
0.03
0.02
0.01
0
-0.01
-0.02
-0.03
δA_pol
50
100
150
200
250
m_3/2 (GeV)
M_1 = m_3/2
M_1 = -m_3/2
C_β = 1/√2
M_2 = M_1
σ(A_pol) = ±0.003
1
M_t = 230 GeV
M_t = 130
M_t = 30
7 - 84
4842A8

Fig. 7

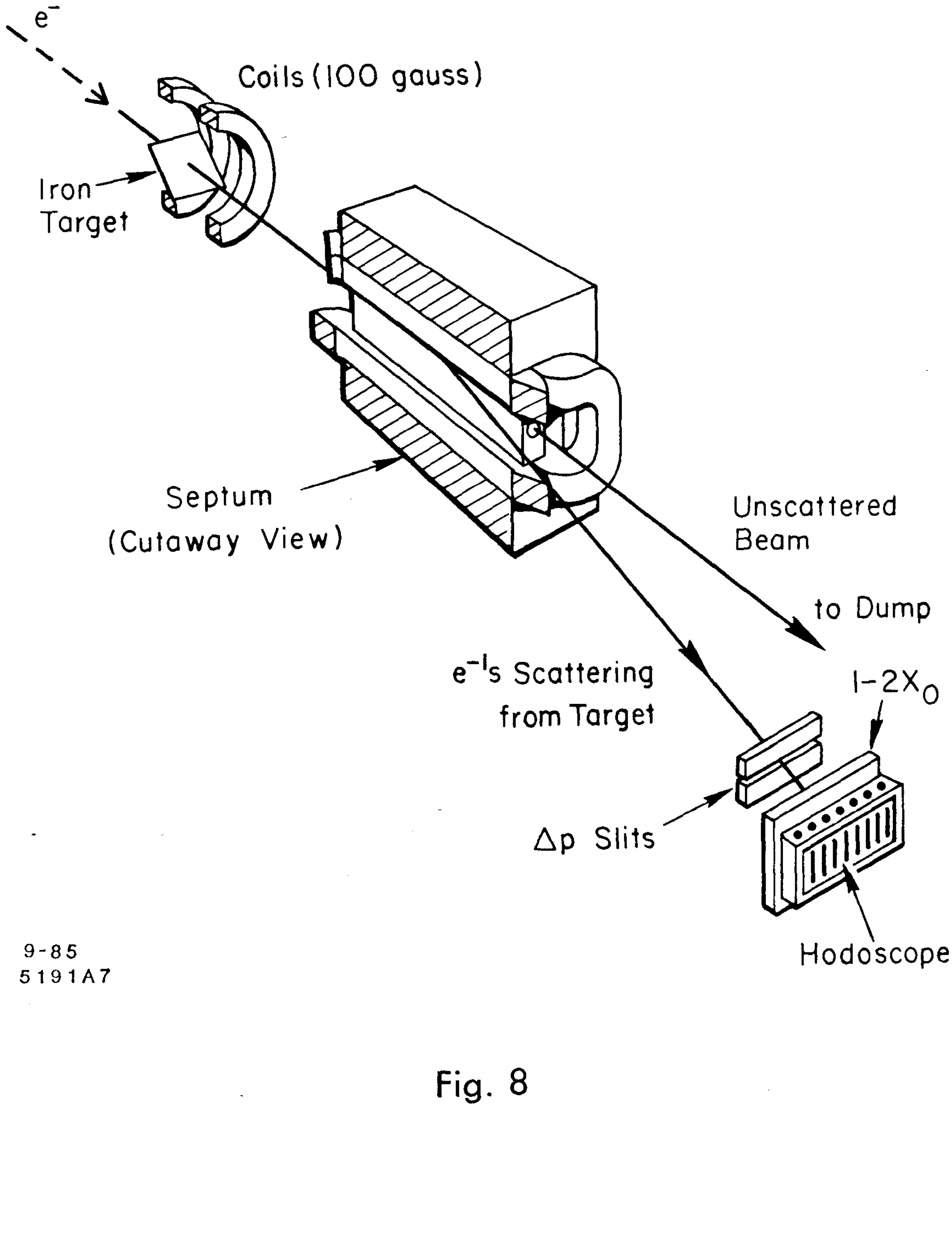
e⁻
Coils (100 gauss)
Iron
Target
Septum
(Cutaway View)
Unscattered
Beam
to Dump
e⁻'s Scattering
from Target
1-2X0
Δp Slits
Hodoscope
9-85
5191A7

Fig. 8

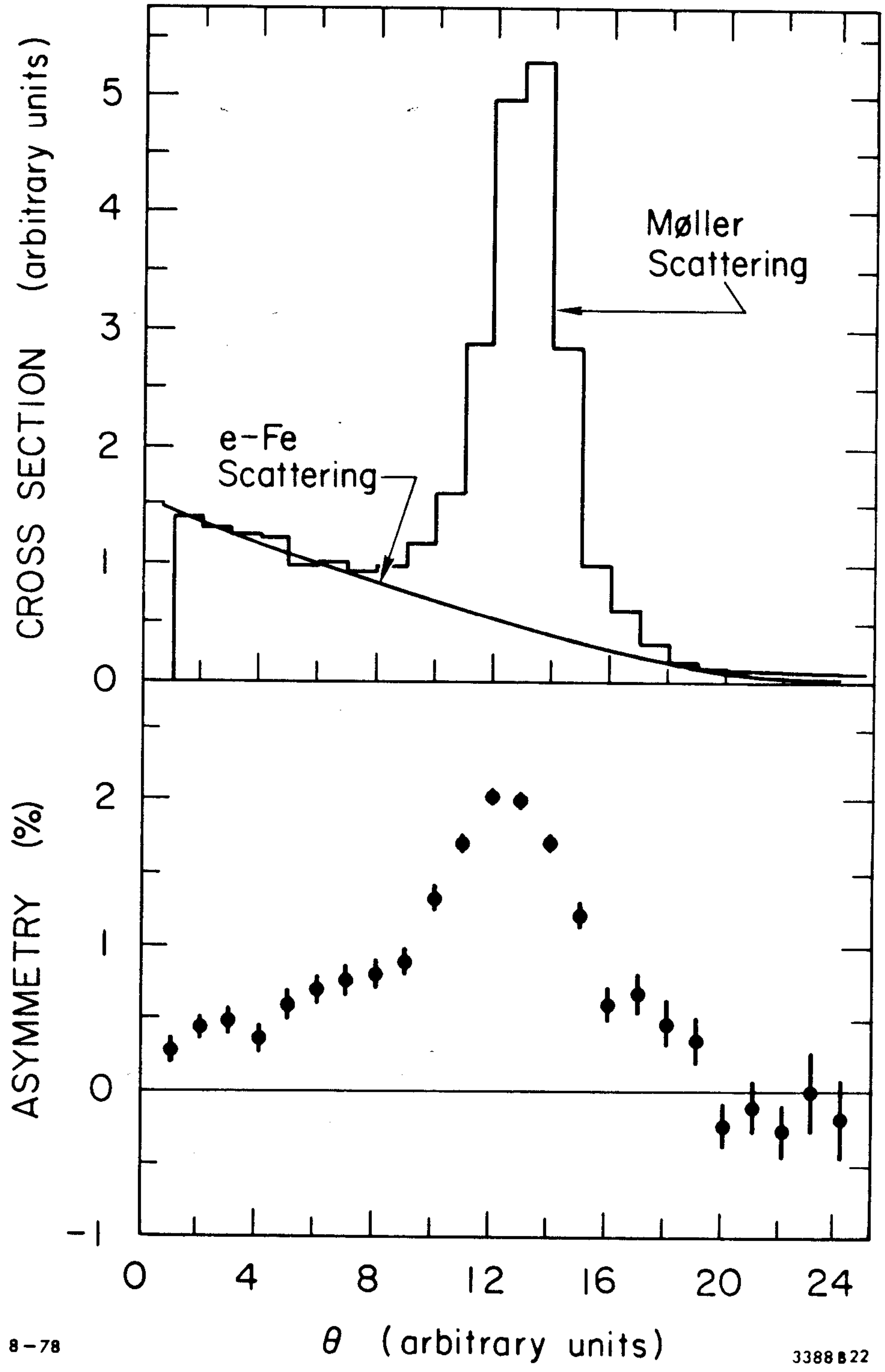
CROSS SECTION (arbitrary units)
ASYMMETRY (%)
Møller Scattering
e-Fe Scattering
0
1
2
3
4
5
-1
0
4
8
12
16
20
24
θ (arbitrary units)
8-78
3388B22

Fig. 9

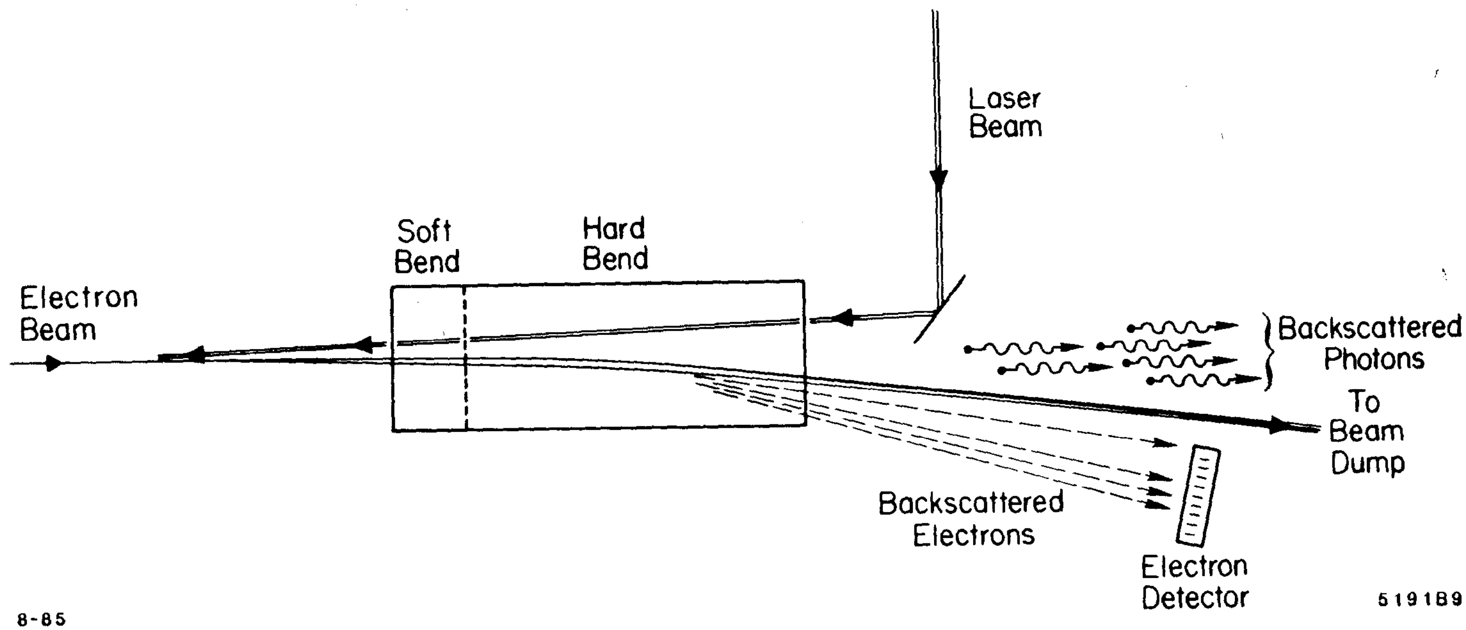
Laser
Beam
Soft
Bend
Hard
Bend
Electron
Beam
Backscattered
Photons
To
Beam
Dump
Backscattered
Electrons
Electron
Detector
8-85
5191B9

Fig. 10